

LATTICE BOLTZMANN METHOD SIMULATION OF THE GAS HEAT CONDUCTION OF NANOPOROUS MATERIAL

by

Ya Fen HAN*, **Shuai LI**, **Hai-Dong LIU**, and **Weipeng CUI**

School of Energy and Power Engineering, Northeast Electric Power University, Jilin, China

Original scientific paper
<https://doi.org/10.2298/TSCI180906102H>

In order to deeply investigate the gas heat conduction of nanoporous aerogel, a model of gas heat conduction was established based on microstructure of aerogel. Lattice Boltzmann method was used to simulate the temperature distribution and gas thermal conductivity at different size, and the size effects of gas heat conduction have had been obtained under micro-scale conditions. It can be concluded that the temperature jump on the boundary was not obvious and the thermal conductivity remained basically constant when the value of Knudsen number was less than 0.01; as the value of Knudsen number increased from 0.01 to 0.1, there was a clear temperature jump on the boundary and the thermal conductivity tended to decrease and the effect of boundary scattering increased drastically, as the value of Knudsen number was more than 0.1, the temperature jump increased significantly on the boundary, furtherly, the thermal conductivity decreased dramatically, and the size effects were significantly.

Key words: nanoporous materials, gas heat conduction,
lattice Boltzmann, size effects

Introduction

Aerogel, a typical nanoporous material, consists of 3-D network skeletons which composed of interconnected spherical solid nanograins and the airs which are filled into the numerous nanopores. Thus, aerogel exhibits a unique combination of properties including high porosity, high surface area and extremely low thermal conductivity [1]. Aerogel has two main advantages which are excellent performance of thermal insulation and lightweight. So, it has been applied to many fields, such as space vehicles, aerogel-filled windows, building envelope materials and others [2]. The mechanisms of the heat transfer in aerogel are generally attributed to three modes which are solid heat conduction, gas heat conduction and thermal radiation [3]. The gas heat conduction is much larger than other two heat transfer modes in the heat transfer process, and its contribution can reach 50% to 80%. Furthermore, the pores of aerogel are mostly in the micro/nano scale, the gas heat conduction belongs to the heat transfer of micro/nano scale. They result in a great challenge to the classical heat conduction theory based on the Fourier law. Therefore, in order to optimize structure and improve thermal properties of aerogel, it is great significance to study the mechanism of gas heat conduction at the micro/nano scale.

At present, the research's on the gas heat conduction properties of aerogel are mainly focused on three aspects, which are experimental measurement, theoretical analysis

* Corresponding author, e-mail: hanyafen@126.com

and numerical simulation [4]. The experimental measurement method is a very intuitive way to reflect the material properties under different conditions, but it is very difficult to directly measure the gas thermal conductivity at the micro/nano scale. In addition, the measurement standards are not uniform that leads to poor accuracy and applicability. For instance, Fricke *et al.* [5] acquired the gas thermal conductivity of aerogel from the total thermal conductivity of experiment and fitted it into a power function which is relation of the material density, the theoretical analysis methods mainly apply three models about gas heat conduction, which are Kaganer model [6], double-pore distribution model [7] and Zeng model [8]. The numerical simulations have been widely applied in the fields of heat transfer of micro/nano scale in recent years. This method cannot only break through the limitations of experimental measurement method, but also can make up for defects of the theoretical analysis method. It can reveal the intrinsic behavior and heat transfer characteristics of the gas molecules in porous materials. Traditional simulation methods include Monte Carlo (MC) and molecular dynamics (MD). To obtain the sampling value of the random variables, a random model need be established and a large number of random experiments are carried out in the MC method. Then, the statistical method is used to obtain the solution of the problem [9]. The MD method need to research a series of the simulated molecules interacting with each other in a certain time and space, and the macroscopic behavior of the system is revealed by studying the motion laws of many single molecules [10]. For example, Zhu *et al.* [11] adopted the MC method to simulate heat transfer of argon in nanoscale, it was found that the gas heat conduction has a significant scale effect when the Knudsen number is very large. Guo *et al.* [12] applied MD method to simulate the movement of argon molecules in aerogel by equilibrium molecular dynamics (EMD) and non-equilibrium molecular dynamics (NEMD), and analyzed their energy transport characteristics. But the two methods could not give the specific temperatures distributions.

The lattice Boltzmann method (LBM), a mesoscopic simulation method developed at the end of the last century, has the advantages of good parallelism, simple boundary processing and easy implementation of the program, and there will not the problem of high computational cost and statistical noise in traditional simulation methods [13]. In addition, it can show the temperature distribution of the gas heat conduction at the micro/nano scale, which cannot be obtained by traditional simulation methods. Therefore, it has been widely applied to the fields of heat transfer.

The gas heat conduction models were built within aerogel in this paper. Its internal temperature distributions and the thermal conductivities were obtained through LBM. Finally, the size effects of the gas heat transfer were deeply discussed at the micro/nano scale.

Physical and mathematical models

The 3-D physical model

Figure 1 displays the model of gas heat conduction of aerogels. We did not consider the influence of solid skeleton and the air was filled in the model. The length, width and height of the model were expressed as L_x , L_y and L_z , respectively. The front and back walls are kept at a constant temperature; the temperature of front wall is $T_2 = 301$ K, and the temperature of back wall is $T_1 = 300$ K, the other four walls were kept adiabatic. The oblique part of the model $y = L_y/2$ ($0 \leq x \leq L_x$, $0 \leq z \leq L_z$) was the middle section, and the dotted line was the middle line in the model. The heat flow was transferred from the high temperature wall (front wall) to the low temperature wall (back wall) along the x -axis.

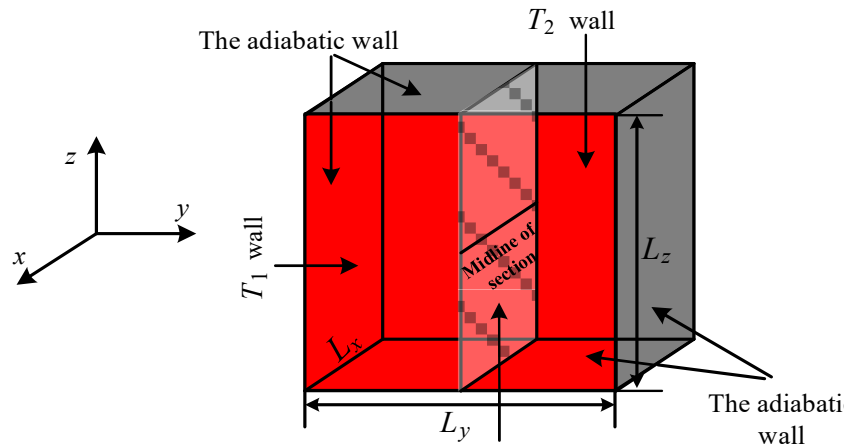


Figure 1. Gas heat conduction model

Mathematical model

The LBM model

The 3-D fifteen-speed (D3Q15) lattice Boltzmann model was used to solve the gas heat conduction of aerogel. The evolution equation was:

$$f_i(r + e_i \delta t, t + \delta t) - f_i(r, t) = -\frac{1}{\tau} [f_i(r, t) - f_i^{eq}(r, t)] \quad (1)$$

where subscript i is the discrete velocity directions of lattice point, r – the space position vector, t was the time, δt – the time step, e_i – the discrete lattice velocity, fig. 2, τ – the dimensionless relaxation time, f_i and f_i^{eq} are, respectively, the internal energy distribution function and corresponding equilibrium distribution function.

$$f_i^{eq} = \begin{cases} (2/9) \rho c_p T, & i = 0 \\ (1/9) \rho c_p T, & i = 1 \sim 6 \\ (1/72) \rho c_p T, & i = 7 \sim 14 \end{cases} \quad (2)$$

where T is the temperature, ρ – the air density, and c_p – the specific heat capacity of air.

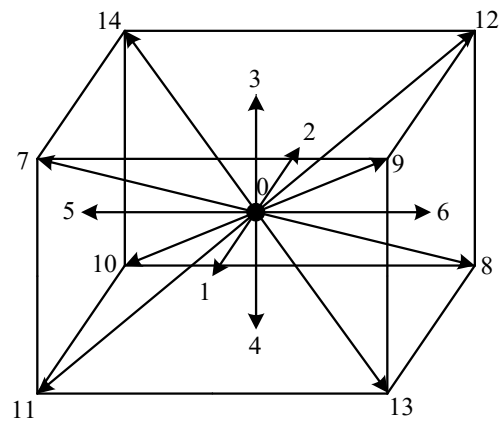


Figure 2. The discrete speed direction of the D3Q15 model

$$e_i = \begin{cases} (0,0,0)c, & i = 0 \\ (\pm 1, \pm 1, 0)c, (\pm 1, 0, \pm 1)c, (0, \pm 1, \pm 1)c, & i = 1 \sim 6 \\ (\pm 1, \pm 1, \pm 1)c, & i = 7 \sim 14 \end{cases} \quad (3)$$

$$\tau = \frac{9}{5} \frac{\lambda}{\rho c_p c^2 \delta t} + 0.5 \quad (4)$$

where λ is the thermal conductivity of the air, c – the lattice speed that theoretically could take any positive value only to insure the τ value within (0.5,2), $c = \delta x / \delta t$ – the space step [14, 15].

Temperature T and heat flux q could be obtained, respectively, according to the following formula:

$$T = \frac{1}{\rho c_p} \sum_i f_i \quad (5)$$

$$q = \left(\sum_i e_i f_i \right) \frac{\tau - 0.5}{\tau} \quad (6)$$

When the temperature got to equilibrium state, the effective thermal conductivity could be calculated on the temperature and heat flux:

$$\lambda_{\text{eff}} = \frac{L_x \int q dA}{\Delta T \int dA} \quad (7)$$

where L_x is the characteristic scale along the direction of the heat flow and dA was the cross-sectional area for the heat flow.

Boundary conditions

In the LBM, for calculation accuracy, stability and computational efficiency, the boundary conditions should be reasonably selected according to the actual situation [16]. Since the influences of solid skeleton were not taken into account in the gas heat conduction, the mirror bounce format was adopted for no friction losses. The energy distribution function could free transfer in this boundary condition. That was equivalent to removing the boundary, and the results would not be affected by the width L_y , and the height L_z . The specific forms were implemented as:

$$f_{i'}(r_b, t) = f_i(r_f, t) \quad (8)$$

where r_b is the boundary lattice point, $r_f = r_b - e_i \delta t$ – the internal lattice point, and $f_{i'}$ – the mirror-symmetric distribution function of f_i . The f_i could be obtained by the inner lattice points that was adjacent the boundary wall.

Program verification

The gas thermal conductivity of aerogel was numerically simulated within 10~80 nm pore sizes, and compared with the results of the Zeng model and inference [17] in the same conditions. The fig. 3 showed that the results of this paper were the similar to the Zeng model but were slightly smaller than it. The Lennard-Jones (LJ) interaction potential of MD was applied in [17]. Because of the potential was weak and it only considered pairwise interaction between atoms. As a result, the simulation results deviated from this paper in 60~70 nm. But they have the same change trend. So, the reliability of the LBM program could be proved

Results and discussion

Gas heat conduction boundary temperature jump

The Knudsen number $Kn(= \lambda/D)$ was the ratio of the mean free path $\lambda(70 \text{ nm})$ of the gas molecules to the characteristic scale D of the pores, it was an important criterion of the micro/nano heat transfer characteristics [16].

When the pore characteristic size was in micro/nano scale, especially close to the mean free path of gas molecules, the scattering effect would occur at the boundary and become an important factor affecting the heat transfer. Figure 4 displayed the variation of the boundary temperature jumps at different Knudsen number along the middle line in the model. The ΔT indicates the sum of value of the boundary temperature jumps. It can be seen from the fig. 4 that the boundary temperature jumps gradually increased with the Knudsen number increasing. When Knudsen number was in 0.1~10, the temperature jump increasing was sharp, and then it gradually tends gentle after the point $Kn = 4$. This was because as the pore characteristic size decreases, the restricting to the gas molecules moving was not obvious at the beginning. When the size was close to the mean free path of the gas molecules, the boundary effects on the molecule moving were strongly. The effects were more sharply with the size decreasing again. Furthermore, the gas molecules could not carry energy, the characteristic of heat diffusion belonged to ballistic transport, and the temperature jumps got to the peak.

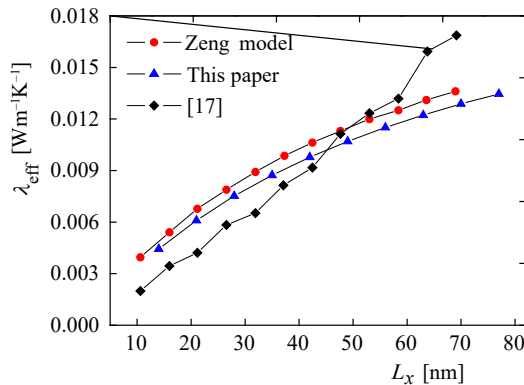


Figure 3. Verification of numerical simulation results

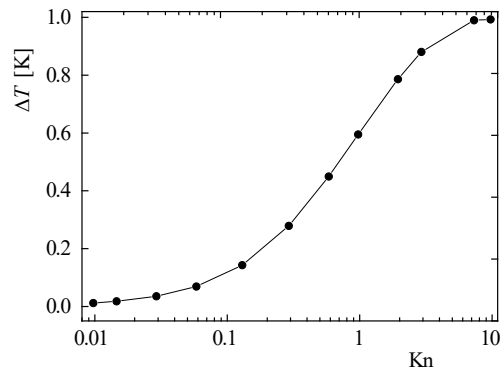


Figure 4. Different Knudsen number temperature boundary temperature jumps

Influence of Knudsen number on gas heat conduction

Figure 5 displayed the temperature the dimensionless steady-state temperature distribution with the dimensionless size at different Knudsen number along the middle line in the model. Where the temperature and pore size were defined $T^* = (T - T_1)/(T_2 - T_1)$, $x^* = x/L_x$. It can be revealed from the graphic that the boundary temperature jumps were most obviously when the Knudsen number was equal to 100. This was because the pore size was very small and the free movement of gas molecules were severely restrained. That was the high temperature boundary molecules could not fully move to transfer the energy to other molecules. When *Knudsen number* = 1, the pore size was more larger and the moving restriction of the gas molecules was weaker, when $Kn = 0.01$, the pore size was too larger than the mean free path of gas molecules to affect movement of gas molecules by boundary scattering. Therefore, the temperature distribution expressed the macroscopic heat transport properties

The fig. 6 displayed the temperature distribution at different Knudsen number in the cross-section $y = L_y/2$ ($0 \leq x \leq L_x, 0 \leq z \leq L_z$). It could be indicated that the temperature gradients were mainly concentrated on the boundary when $Kn = 100$. The temperature distributions were gradually close to uniform when $Kn = 1, 0.7, 0.01$. Namely, the macroscopic characteristics of thermal transport trended to show and the reasons were to fig. 5.

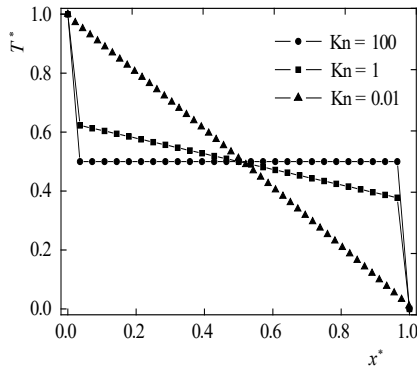


Figure 5. Dimensionless steady-state temperature distribution

Gas thermal conductivity

Since the effects of boundary scattering occurred and the temperature distribution was discontinuous in the gas heat conduction within the micro/nano scale, the Fourier law was no longer applicable. The effective thermal conductivities were calculated by the method in reference [18]. The equation was as follow:

$$\lambda_{\text{eff}} = \frac{qL_x}{\Delta T_{\text{left}} + \Delta T + \Delta T_{\text{right}}} \quad (9)$$

where ΔT_{left} is the value of left boundary temperature jump, ΔT_{right} – the value of right boundary temperature jump, and L_x – the characteristic scale along the direction of the heat flow, fig. 7.

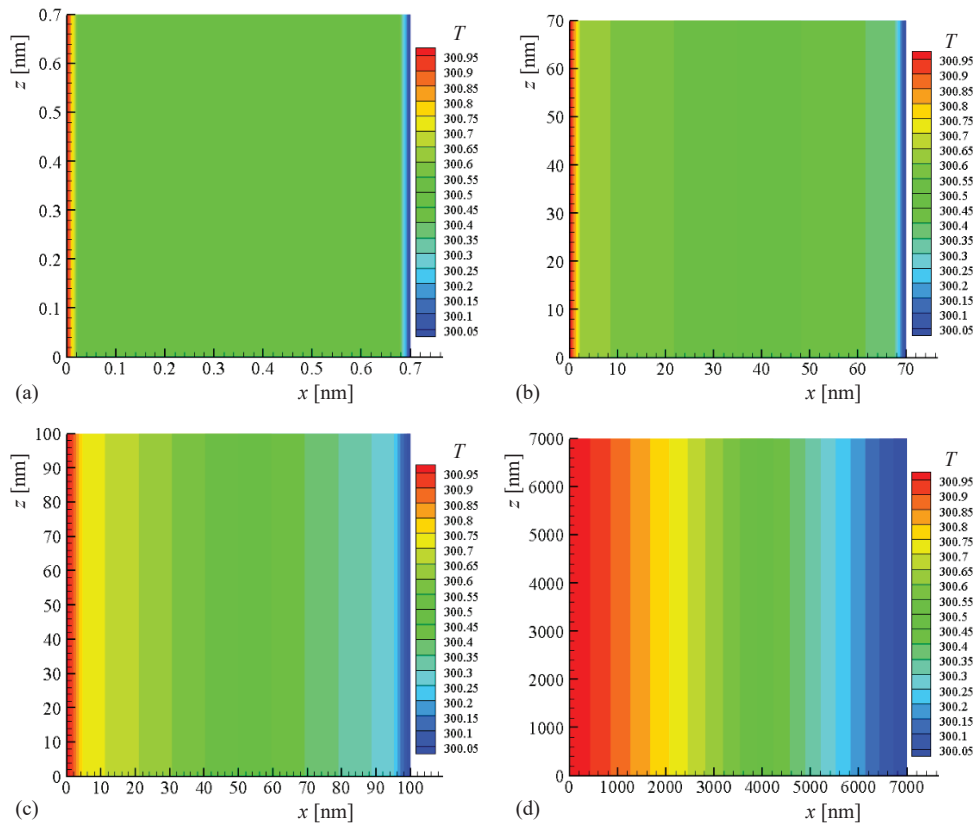


Figure 6. Temperature distribution; (a) Kn = 100, (b) Kn = 1, (c) Kn = 0.7, and (d) Kn = 0.01

The fig. 8 shown that the effective thermal conductivity changing by the size from 10 nm to 7000 nm. The values trended to constant when the pore sizes were from 1000 nm to 7000 nm. But the effective thermal conductivities dramatically decreased when the pore sizes

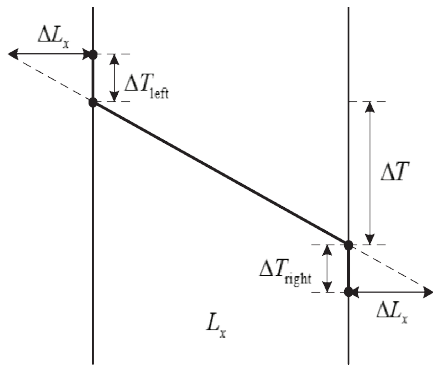


Figure 7. Calculation model of effective thermal conductivity

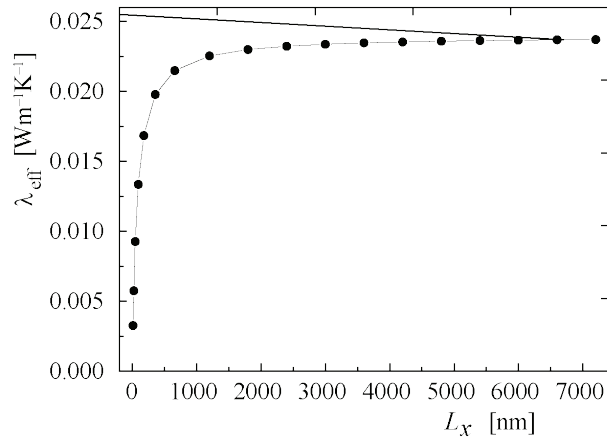


Figure 8. Effective thermal conductivity of gas phase

were little than 1000 nm. The reasons were also similar to temperature changing. Namely the heat transport was restricted when the size decreased near to the mean free path of gas molecules. We know that the gas heat conduction is carried out by the thermal movement of gas molecules, when the pore size was much larger than the mean free path of gas molecules, the gas molecules were not affected by boundary scattering and could move freely, therefore, the system will exhibit macroscopic characteristic of heat conduction; when the pore size gradually decreases, the free movement of gas molecules would be restricted by the boundary, and thermal transport would also gradually weakened between gas molecules, so the thermal conductivity displays an obvious downward trend.

Conclusions

In this paper, the gas heat conduction model of aerogel was established, and the size effects of heat transport were studied deeply by LBM. The results were as follow.

- When the characteristic sizes of pores were much larger than the mean free path of gas molecules ($L_x > 1000$ nm), the gas heat conduction was characterized by macroscopic transport and presents a uniform temperature distribution. And the effective thermal conductivities maintained constant.
- When the pore characteristic sizes were close to or less than the mean free path of the gas molecules (70 nm), the significant temperature jumps occurred on the boundaries. And the effective thermal conductivities would rapidly decrease with the pore size.

Acknowledgment

This work is supported by National Natural Science Foundation of China (Grant No.: 51606034) and the Education Department Foundation of Jilin Province (Grant No.: JJKH20180417KJ), which are greatly appreciated.

Nomenclature

| | | | |
|-------|--|------------|---|
| c_p | – specific heat capacity of air, [$kJkg^{-1}K^{-1}$] | f_i | – internal energy distribution function |
| c | – lattice speed, [ms^{-1}] | f_i^{eq} | – equilibrium distribution function |
| dA | – cross-sectional area for the heat flow, [m^2] | i | – discrete velocity directions of lattice point |
| e_i | – discrete lattice velocity | Kn | – Knudsen number |

| | | | |
|---------------------------|--|----------------------|---|
| q | – heat flux, [Jm^{-1}] | δt | – time step, [s] |
| r_b | – boundary lattice point | <i>Greek symbols</i> | |
| r_f | – internal lattice point | λ | – thermal conductivity of the air [$\text{Wm}^{-1}\text{K}^{-1}$] |
| r | – space position vector | ρ | – air density [kgm^{-3}] |
| T | – temperature, [K] | τ | – dimensionless relaxation time, [s] |
| ΔT_{left} | – value of left boundary temperature jump | | |
| ΔT_{right} | – value of right boundary temperature jump | | |

References

- [1] Han, Y. F., *et al.*, Characteristic of Heat Conduction in Nano-Insulation Material, *Journal of Functional Materials*, 45 (2014), 3, pp. 3017-3019
- [2] Zhang, Z. H., *et al.*, Silica Aerogel Materials: Preparation, Properties, and Applications in Low-Temperature Thermal Insulation, *Journal of Aeronautical Materials*, 35 (2015), 1, pp. 87-96
- [3] Wu, X. D., *et al.*, Advance in Research of High Temperature Resistant Aerogel Used as Insulation Material, *Materials Review*, 29 (2015), 9, pp. 102-108
- [4] He, Y. L., Xie, T., A Review of Heat Transfer Models of Nanoporous Silica Aerogel Insulation Material, *Chinese Science Bulletin*, 60 (2015), 2, pp. 137-163
- [5] Fricke, J., *et al.*, Optimization of Monolithic Silica Aerogel Insulants, *International Journal of Heat and Mass Transfer*, 35 (1992), 9, pp. 2305-2309
- [6] Kaganer, M. G., Moscona, A., Thermal Insulation in Cryogenic Engineering, *Israel Program for Scientific Translations Jerusalem*, 1969
- [7] Reichenauer, G., *et al.*, Relationship between Pore Scale and the Gas Pressure Dependence of the Gaseous Thermal Conductivity [J], *Colloids and Surfaces A: Physicochem. Eng. Aspects*, 300 (2007), 1, pp. 204-210
- [8] Zeng, S. O., *et al.*, Geometric Structure and Thermal Conductivity of Porous Medium Silica Aerogel, *Journal of Heat Transfer*, 117 (1995), 4, pp. 1055-1058
- [9] Zhu, L. L., The Monte Carlo Method and Application, M. Sc. thesis, Central China Normal University, Wuhan, China, 2014
- [10] Hui, Xie, Chao L., Molecular Dynamics Simulations of Gas Flow in Nanochannel with a Janus Interface, *AIP Advances*, 2, (2012), 042126
- [11] Zhu, C. Y., *et al.*, The DSMC Study on Gas Heat Conduction in Nanoscale, *Journal of Engineering Thermophysics*, 37 (2016), 5, pp. 1027-1031
- [12] Guo, Y. H., *et al.*, Molecular Dynamics Study on Heat Conductivity Mechanism of Silica Aerogel, *Journal of Engineering Thermophysics*, 32 (2011), 1, pp. 107-110
- [13] He, Y. L., *et al.*, Lattice Boltzmann Method and Its Applications in Engineering Thermophysics, *Chinese Science Bulletin*, 54 (2009), 18, pp. 2638-2656
- [14] Wang, J., *et al.*, A Lattice Boltzmann Algorithm for Fluid–Solid Conjugate Heat Transfer, *International Journal of Thermal Sciences*, 46 (2007), 3, pp. 228-234
- [15] Wang, M., Pan, N., Predictions of Effective Physical Properties of Complex Multiphase Materials, *Materials Science & Engineering R*, 63 (2009), 1, pp. 1-30
- [16] He, Y. L., *et al.*, Lattice Boltzmann Method: Theory and Applications, Science Press, Beijing, 2009
- [17] Ge, C. X., Investigation of Gas Thermal Conductivity in Nanopore by Molecular Dynamics, Ph. D. thesis, Harbin Institute of Technology, Harbin, China, 2010
- [18] Han, Y. F., *et al.*, Simulation on Phonon Heat Transport of Silicon Dioxide Nanomaterial by Lattice Boltzmann Method, *Journal of Engineering Thermophysics*, 32 (2011), 9, pp. 1571-1574